Astronomical Journal, Accepted 2005 April 13th
Preprint typeset using LaTeX style emulateapj v. 6/22/04

THE *GALEX* ULTRAVIOLET VARIABILITY (GUVV) CATALOG

Barry Y. Welsh,[1] Jonathan M. Wheatley,[1] Kenneth Heafield,[2] Mark Seibert,[2] Stanley E. Browne,[1] Samir Salim,[3] R. Michael Rich,[3] Tom A. Barlow,[2] Luciana Bianchi,[4] Yong-Ik Byun,[5] Jose Donas,[6] Karl Forster,[2] Peter G. Friedman,[2] Timothy M. Heckman,[4] Patrick N. Jelinsky,[1] Young-Wook Lee,[5] Barry F. Madore,[7] Roger F. Malina,[6] D. Christopher Martin,[2] Bruno Milliard,[6] Patrick Morrissey,[2] Susan G. Neff,[8] David Schiminovich,[2] Oswald H. W. Siegmund,[1] Todd Small,[2] Alex S. Szalay,[4] and Ted K. Wyder[2]

Astronomical Journal, Accepted 2005 April 13th

ABSTRACT

We present Version 1.0 of the NASA Galaxy Evolution Explorer (*GALEX*) ultraviolet variability catalog (GUVV) that contains information on 84 time-variable and transient sources gained with simultaneous near and far ultraviolet photometric observations. These time-variable sources were serendipitously revealed in the various 1.2° diameter star fields currently being surveyed by the *GALEX* satellite in two ultraviolet bands (NUV 1750 - 2750 Å, FUV 1350 - 1750 Å) with limiting AB magnitudes of 23 - 25. The largest-amplitude variable objects presently detected by *GALEX* are M-dwarf flare stars, which can brighten by 5 - 10 mag in both the NUV and FUV bands during short duration (< 500 s) outbursts. Other types of large-amplitude ultraviolet variable objects include *ab*-type RR Lyrae stars, which can vary periodically by 2 - 5 mag in the *GALEX* FUV band. This first GUVV catalog lists galactic positions and possible source identifications in order to provide the astronomical community with a list of time-variable objects that can now be repeatedly observed at other wavelengths. We expect the total number of time-variable source detections to increase as the *GALEX* mission progresses, such that later version numbers of the GUVV catalog will contain substantially more variable sources.

Subject headings: stars: variables: other (dMe) — stars: variables: other (RR Lyrae) — ultraviolet: stars

1. INTRODUCTION

The primary scientific mission of the NASA Galaxy Evolution Explorer (*GALEX*) satellite (Martin et al. 2005) is to explore star formation processes and the histories of galaxies through imaging photometric observations in two ultraviolet bands (NUV 1750 - 2750Å FUV 1350 - 1750Å). However, *GALEX* is also making serendipitous ultraviolet photometric measurements of several million stars and other non-galactic objects during the course of its All-Sky Imaging Survey (AIS) and during its deeper repeated observations of selected small areas of the sky with its Deep Imaging Survey (DIS) and Medium Imaging Survey (MIS). In particular, *GALEX* has a high sensitivity, low background noise, a wide field of view (1.°2), and it makes repeated visits to deep fields (Morrissey et al. 2005). These observational capabilities have enabled the detection of numerous variable and transient ultraviolet sources, many of which exhibit much larger amplitudes of variation in the ultraviolet region than that recorded at visible wavelengths.

One good example of a serendipitous source-detection by *GALEX* is the RR Lyrae star, ROTSE-I J143753.84+345924.8 (Wheatley et al. 2005). Using a series of 38 separate *GALEX* pointings a 4.9 AB magnitude variation was observed in the FUV band, compared with only a 0.8 magnitude variation at visible wavelengths. From these ultraviolet light-curves it was possible to constrain theoretical models that placed meaningful limits on both the temperature and metallicity of the star. One further example of a *GALEX* serendipitous observation is that of the massive ultraviolet flare on the dM4e star, GJ 3685A, in which an overall brightness increase of AB > 4 magnitudes was observed in both the FUV and NUV bands in a time period of only 60 seconds (Robinson et al. 2005). Other types of astronomical source that *GALEX* can potentially detect are cataclysmic variables, Cepheid variables, soft X-ray transients and (possibly) gamma-ray bursters.

In this Paper we list 84 variable and transient ultraviolet sources that have been detected during the first 15 months of the *GALEX* all-sky survey, which is currently envisaged to be completed within the next 18 months. These present observations (taken from data covering ∼ 10% of the sky) will form the basis of an increasing database of variable UV sources whose physical properties can be further explored in more detail by the astronomical community in other wavelength bands.

2. OBSERVATIONS AND DATA ANALYSIS

We have used the *GALEX* FUV and NUV-band photometric imaging data recorded during the period

[1] Experimental Astrophysics Group, Space Sciences Laboratory, University of California, 7 Gauss Way, Berkeley, CA 94720; bwelsh@ssl.berkeley.edu, wheat@ssl.berkeley.edu
[2] California Institute of Technology, MC 405-47, 1200 East California Boulevard, Pasadena, CA 91125
[3] Department of Physics and Astronomy, University of California, Los Angeles, CA 90095
[4] Center for Astrophysical Sciences, The Johns Hopkins University, 3400 N. Charles St., Baltimore, MD 21218
[5] Center for Space Astrophysics, Yonsei University, Seoul 120-749, Korea
[6] Laboratoire d'Astrophysique de Marseille, BP 8, Traverse du Siphon, 13376 Marseille Cedex 12, France
[7] Observatories of the Carnegie Institution of Washington, 813 Santa Barbara St., Pasadena, CA 91101
[8] Laboratory for Astronomy and Solar Physics, NASA Goddard Space Flight Center, Greenbelt, MD 20771

June 2003 to August 2004, which reside in the Multi-Misison Archive at the Space Telescope Science Institute (MAST). During this time-period the *GALEX* satellite performed several types of imaging and spectroscopic observations using its 1.2° field of view. We have restricted our analysis to data recorded in the photometric imaging mode by the two FUV and NUV photon-counting detectors (Jelinsky et al. 2003). These imaging observations consist of data recorded in three observational modes, each with different exposure times. They consist of (i) the All-Sky Imaging Survey (AIS) which observes regions of the sky for $\sim$ 100 seconds. Adjacent AIS sky-fields have a small (2%) area of overlap that enables a limited number of detections of source variability between consecutive survey images, (ii) the Medium Imaging Survey (MIS), which observes regions of the sky with a total exposure of $\sim$ 1500 seconds (i.e. one *GALEX* orbit), that in some cases have been repeatedly observed in order to gain a better resultant S/N ratio of the sky-field, and (iii) the Deep Imaging Survey (DIS) which repeatedly observes specific pre-selected regions of interest on the sky for many ($>$ 20) orbits in order to accumulate a total exposure time of $\sim$ 30,000 seconds for each selected sky-field. In addition to these 3 main types of survey mode, *GALEX* is also carrying out a survey of bright nearby galaxies (NGS), which entails recording both photometric imaging and spectroscopic data on selected fields for periods typically of $\sim$ 2000 seconds. In Table 1 we list the total area of the sky (in square degrees) observed thus far by the various *GALEX* surveys, together with the respective number of variable sources detected. Not surprisingly, the largest number of variable source detections per unit area have been found in the Deep Imaging Survey mode (i.e. about one source per field).

All of these currently observed sky-fields are located well away from the galactic plane in order to avoid saturation of the detectors due to overly-bright stellar sources and to avoid regions where interstellar absorption is high. The recorded data files contain photon events that have been processed by the standard *GALEX* Data Analysis Pipeline operated at the Caltech Science Operations Center (Pasadena, CA) that ingests time-tagged photon lists, instrument and spacecraft housekeeping data and satellite pointing aspect information (Morrissey et al. 2005). The data pipeline uses a source detection algorithm (called Sextractor) to produce a catalog of source positions and corresponding ultraviolet magnitudes for each observation. Comparison software was then run on this catalog to detect sources that we deem as being either variable or transient. Variable sources are defined as being present in repeatedly observed fields and exhibiting an orbital variation greater than AB = 0.3 magnitudes (with an associated change $> 3\sigma$ in the magnitude error) in their derived FUV and/or NUV magnitudes recorded in two or more separate observations. Transient sources are defined as objects which are detected only once, in the FUV and/or NUV bands, in a repeatedly observed star-field. We note that a 'transient source' may be a variable star detected only once near maximum light.

In Table 2 we list 84 sources that have been identified as being either variable (V) or transient (T) events by the aforementioned *GALEX* ultraviolet sky-field observations. We have not included several asteroids that appeared as potential transient UV objects in the data. The catalog number of each of the detected sources is listed in column (1) of this Table. This number is a unique identifier containing both the Right Ascension (J-2000.0) of the source in hours, minutes and decimal seconds and the corresponding source Declination (J-2000.0) in degrees, minutes and decimal seconds. These positions are typically accurate to $\pm$ 1.0 arc sec for sources that have been observed in the central 1° of the detectors (Morrissey et al. 2005). In column (2) we list whether the source is variable (V) or transient (T), based on the citerion listed in the previous paragraph. Column (3) lists the USNO-B1.0 all-sky catalog designation (Monet et al. 2003), where available, for the source that is closest (and within $\pm$5 arc seconds) to the position of the object listed in column (1). In column (4) we provide a possible identification for the source based on objects listed in the Simbad on-line astronomical catalog for targets with positions that are coincident within $\pm$5 arc sec of the *GALEX* determined position, and in column (5) we list the most likely type of astronomical source-type for that object. Criteria used to make this latter determination are generally varied, but (for the brighter sources) are mainly based on either their Simbad catalog identifications or on inspection of their *GALEX* UV light-curve data. Flare stars were found to be generally bright just once during a series of UV observations, whereas periodic variables (PVs) exhibited a large range of values in their measured UV magnitudes. Some of these PVs are listed as RR Lyrae stars in Simbad and such designations have been used accordingly in column (5).

In Column (6) we list the *GALEX* survey mode (AIS, MIS, DIS or NGS) of the sky field in which the object was discovered. Columns (7) and (8) respectively list the total number of observations of the particular sky field in the NUV channel and the number of these exposures in which the source was detected. Column (9) lists the maximum observed NUV magnitude for the source (measured over one AIS, MIS, DIS or NGS integration period) and column (10) lists the variation between the correspondingly measured maximum and minimum NUV magnitudes (i.e. Δm). Similarly, columns (11) - (14) list the equivalent number of observations, number of detections, maximum magnitude and variation in magnitude for the FUV channel. Here we note that the non-detection of a source previously observed in both (or one) of the two UV-bands can be attributed to either intrinsic variability (i.e. an astrophysical effect) or by the fact that one of the detectors was turned off during a particular observation for instrument safety reasons. Finally, columns (15) and (16) list the respective g and r magnitudes as recorded by the Sloan Digital Sky Survey (SDSS) catalog (Abazajian et al. 2003) for the source designation listed in column (3). Stars with uncertain SSDS magnitudes (due to detector saturation and other effects) are marked with an asterisk (*). We also note that as the data pipeline software matures and refines over the extent of the *GALEX* mission, the derived NUV and FUV source magnitude values may alter slightly. It is hoped that later versions of the GUVV catalog, based on the entire *GALEX* data archive, will be forthcoming.

3. DISCUSSION

The 84 *GALEX* variable and transient sources listed in Table 2 have been observed using $\sim$ 2600 separate ob-

TABLE 1
GALEX SURVEY INFORMATION

Survey Mode	Square Degrees Surveyed	Number of Variable Sources Detected	Detections per Square Degree
AIS	2729	52	0.02
MIS	129	13	0.10
DIS	15	18	1.2
NGS	49	8	0.16

servations that cover a total of ∼ 3000 sq. degrees of sky. Variable sources (72) account for 86% of the listed sources and the remaining 12 sources are all of a transient nature. Only one of the sources, J090054.7+303113.3, was detected as being simultaneously transient in *both* of the FUV and NUV channels. The remaining transient sources were singularly detected in only one of the two *GALEX* channels, presumably due to the different sensitivity limits of each UV photometric band.

Several of the GUVV sources are previously known flare stars, RR Lyrae stars, quasars or X-ray sources, but the large majority of the UV variable objects in this catalog have no previously listed source identification. We note that Siebert et al. (2005) have produced color-color diagrams for $> 350{,}000$ (non-variable) objects detected by *GALEX* in a 143 sq. degree portion of the sky that overlaps with that of the Sloan Digital Sky Survey (SDSS) (Abazajian et al. 2003). Plots of (g - r) versus (m_{nuv} - g) magnitude have revealed a segregation of main sequence, horizontal branch, white dwarf, subdwarf and M dwarf stellar populations in the *GALEX* data. It has been found that the number density of M dwarf - white dwarf binary systems is at least twice as high in the *GALEX* NUV data than that found using the SSDS u-magnitude. In order to assess if there are any similar underlying fundamental observable parameters that may classify these 84 detections into distinct variable source sub-groups we have produced the following Figures in which the data have been plotted with 3 different symbols identified with known flares stars (open circles), known RR Lyrae stars (filled circles) and and sources with no identification (crosses).

In Figure 1 we plot values of (g - r) versus (m_{fuv} - g) magnitude and see that the vast majority of the data points divide into two separate groupings with (i) $0.4 > (g - r) > -0.2$ and (ii) $1.6 > (g - r) > 1.0$. The former data group (in the lower region of Figure 1) contains all of the identified RR Lyrae stars in the *GUVV* catalog and the latter data grouping (in the upper region of Figure 1) contains two dMe flare stars. With regard to the former data group we note that Ivezic et al. (2005) have found very similar color-color limits for RR Lyrae stars based solely on their SSDS (g - r) magnitudes. Since all of the data points contained in Figure 1 are targets that have been deemed to be variable based on their *GALEX* UV observations, then the un-identified sources in the lower region of this figure are most probably also RR Lyrae (or δ Sct) type stars. We are currently obtaining low resolution visible spectra of the un-identified sources in the upper region of Figure 1 to determine if they are dMe flare stars. If the stars in this regime do turn out to be dMe flares then plots like Figure 1 may represent a very useful tool for the future selection of previously unidentified RR Lyrae and dMe flare stars based solely on their *GALEX* UV variability and their SDSS (g - r) magnitudes.

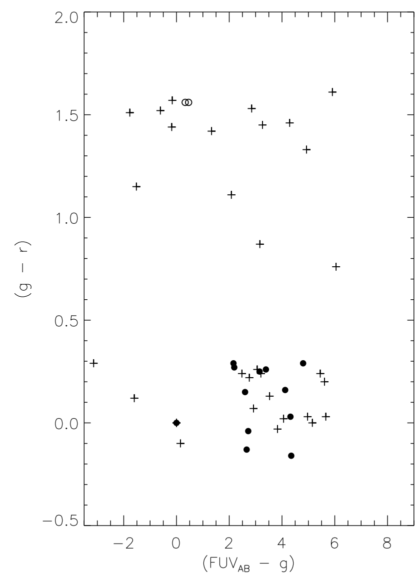

FIG. 1.— Plot of the SDSS (g - r) magnitudes versus (m_{fuv} - g) magnitudes for the GUVV catalog sources. Note the division of the sources into two distinct groups with different (g - r) magnitudes. The lower grouping of targets contains mainly RR Lyrae stars (filled circles) and the upper grouping are probably mostly dMe flare stars (open circles). The remainder of the targets are un-identified GUVV sources (crosses).

In Figure 2 we plot the observed *GALEX* peak FUV magnitude versus the peak NUV magnitude. We see that the majority of these sources lie within ∼ ±1.0 magnitudes of the best-fit straight-line (of slope +0.81). However, three sources, J211517.8+000432.5 (the RR Lyare star, SW Aqr), J114740.7+001521.0 (the dM4 flare star, GJ 3685A) and J141755.4+714107.6 lie well outside of these limits. Apart from the loose proportionality between the FUV and NUV peak magnitudes for all these sources, we see no other underlying physical discriminators in this figure.

3.1. *Interesting GUVV objects*

Of the 26 GUVV sources that possess reliable identifications in column (4) of Table 2, we note that 14 are known RR Lyrae variables, 4 are previously known dMe flare stars, and 5 are radio and/or X-ray sources. The vast majority of the GUVV sources have no firm identification and therefore are clearly prime targets for follow-up ground-based photometric and spectroscopic observa-

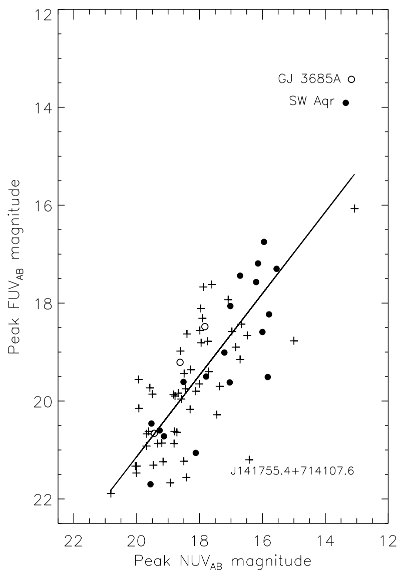

FIG. 2.— Plot of the *GALEX* peak FUV AB magnitude versus the peak NUV AB magnitude for the GUVV catalog sources. The majority of the targets lie within ± 1 magnitude of a straight-line of slope +0.81. The 3 exceptions are highlighted on the figure. See Figure 1 text for an explanantion of the plotting symbols.

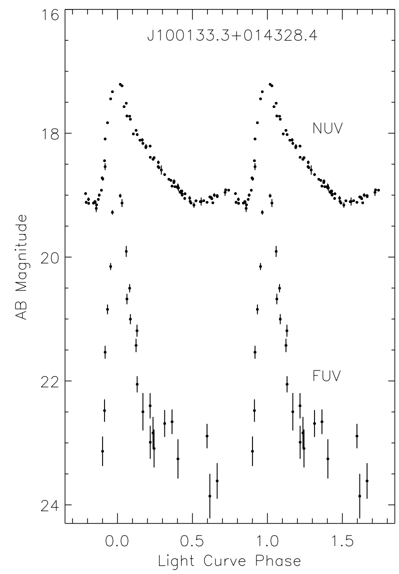

FIG. 3.— Observed *GALEX* FUV and NUV light-curves for the star GUVV-J100133.3+014328.4, which we identify as a new RR Lyrae star. The phase was computed using a derived period of 0.543 days.

tions. To highlight some of the interesting astronomical sources that have thus far been identified in the GUVV catalog, in the following two sections we illustrate some of the scientific studies that can be explored using these new UV data.

3.1.1. *RR Lyrae Stars*

GALEX is well-suited for the detection of RR Lyrae variable stars since they are typically found to vary by 2 - 6 magnitudes in the FUV band, with a corresponding NUV magnitude change of ∼ 50% of this value. This can be compared with a typical change in magnitude of only ∼ 1.0 recorded at visible wavelengths (Skillen et al. 1993). In Figure 3 we show the *GALEX* NUV and FUV light-curves for the star GUVV-J100133.3+014328.4 that show AB magnitude variations of ∼ 4.9 in the FUV band and ∼ 2.0 in the NUV band (Browne 2005). These curves were constructed using a least-string software program that derived a period of 0.543 days for the light-curve from 82 NUV and 26 FUV observations. It is clear from these UV variability data that this star is of the RR Lyrae type (parenthetically we note that its g - r value of 0.03 magnitudes places it in the lower region of Figure 1 together with the other RR Lyrae stars). Since the derived FUV flux from *GALEX* observations of this class of variable star is highly sensitive to a change in the Kurucz model atmosphere temperature of only ∼ 100 - 200K, these UV data taken together with visible light-curve observations can enable better estimates to be made of the stellar metallicity. However, although a large flux variation can be observed from RR Lyrae stars in the FUV (and NUV), the current sensitivity limit of the *GALEX* observations for these faint sources presently limits their potential use as (non-galactic) cosmic distance scale indicators. Thus, although *GALEX* may well prove to be a rich source of galactic RR Lyrae star detection, their stellar distances are probably better determined using follow-up visible observations with large aperture ground-based telescopes.

3.1.2. *Flare Stars*

GALEX has been fortunate to detect many large short-lived outbursts of UV flux, typically lasting < 200 seconds, generated by dMe-type flare stars. This emission is linked to magnetic processes occurring in their outer stellar atmospheres (coronae). In one extreme case of the dM4e star GJ 3685 (GUVV-J114740.7+001521.0), its overall UV brightness increased by more than a factor of 10,000 making it 20 times larger than any previously observed UV flare (Robinson et al. 2005). It should be noted that the changes in the FUV and NUV magnitudes listed in columns (10) and (14) for these events are average values recorded over one *GALEX* observation period. Only through inspection of the individual time-tagged photon events, recorded with a time resolution of 0.005 sec for each of these observational periods, can the underlying physical properties of the flare-mechanism be revealed. In the case of the previously mentioned UV flare, the *GALEX* observations have detected two major outburst events separated by 200 seconds that were accompanied by numerous short-duration (< 10 sec) micro-flares during the entire 1600 second observation. In Figure 4 we show the NUV light curve (gained from time-tagged photon data) for the flare recorded by *GALEX* on the star GUVV-J144738.47+035312.1 on June 3rd 2004, that shows a more modest brightness increase that consists of at least 4 major outbursts observed during a ∼ 150 second flaring interval. We note that although the brightest flaring M dwarf stars detected by *GALEX* have distances typically < 30 pc and can inject up to ∼ 10^{34} erg into the surrounding interstellar gas, based on the number of these events recorded thus far by *GALEX* this UV flux is insufficient to make a significant contribution to the global ionization properties of the local interstellar medium.

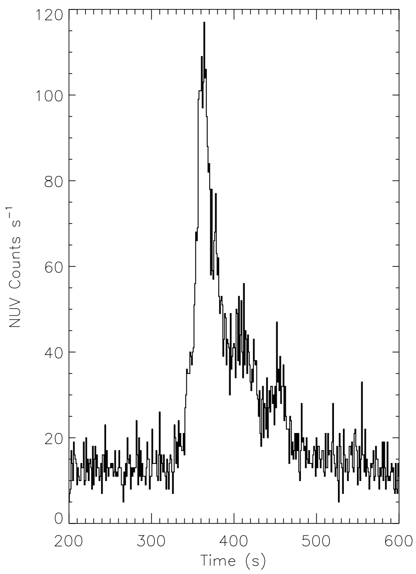

Fig. 4.— Near UV emission as a function of time for the flare recorded on the star GUVV-J144738.47+035312. Note at least two subsidiary emission events that followed within 100 seconds of the main flare.

We gratefully acknowledge NASA's support for construction, operation, and science analysis for the GALEX mission, developed in cooperation with the Centre National d'Etudes Spatiales of France and the Korean Ministry of Science and Technology. We acknowledge the dedicated team of engineers, technicians, and administrative staff from JPL/Caltech, Orbital Sciences Corporation, University of California, Berkeley, Laboratoire d'Astrophysique de Marseille, and the other institutions who made this mission possible. Financial support for this research was provided by NASA grant NAS5-98034. This publication makes use of data products from the SIMBAD database, operated at CDS, Strasbourg, France.

REFERENCES

Abazajian, K., Adelman-McCarthy, J.K., Agueros, M.A. et al., 2003, AJ, 126, 2081

Browne, S.E., 2005, PASP, (submitted)

Ivezic, Z., Vivas, A.K., Lupton, R. and Zinn, R., 2005, AJ, 129, 1096

Jelinsky, P., Morrisssey, P., Malloy, J. et al. 2002, Proc. SPIE, 4854, 233

Martin, D.C., et al. 2005, ApJ, 619, L1

Monet, D.G., Levine, S.E., Canzian, B. et al., 2003, AJ, 125, 984

Morrissey, P., Schiminovich, D., Barlow, T.A. et al. 2005, ApJ, 619, L7

Robinson, R., Wheatley, J.M., Welsh, B.Y. et al. 2005, ApJ, (submitted)

Siebert, M., Budavari, T., Rhee, J. et al., 2005, ApJ, 619, L23

Skillen, I., Fernley, J., Stobie, R. and Jameson, R., 1993, MNRAS, 265, 301

Wheatley, J.M., Welsh, B.Y., Siegmund, O.H.W. et al. 2005, ApJ, 619, L123

Wozniak, P.R., Vestrand, W.T., Akerlof, C.W. et al. 2004, AJ 127, 2436

TABLE 2
GALEX Ultraviolet Variability Catalog, V1.0.

GUVV		USNO-B1.0	ID	Type	Discovery Survey	NUV N_{obs}	N_{det}	Max	Δm	FUV N_{obs}	N_{det}	Max	Δm	SDSS DR3 g	r
J004347.9+421654.9	V	1322-0015866	CC And	Delta Sct variable	NGS	9	9	13.02	0.63	9	9	16.07	0.93	-	-
J004548.2-435509.1	V	0460-0006826		PV	DIS	10	10	16.00	1.38	10	9	18.59	3.77	-	-
J010732.6+360956.5	V	1261-0017670	1RXS J010732.1+361001	x-ray source	NGS	2	2	20.01	0.60	2	2	21.47	0.55	-	-
J085218.1+311047.2	V	1211-0164505			AIS	3	3	15.00	0.33	3	3	18.77	0.37	15.23*	15.19*
J090054.7+303113.3	T	-			AIS	2	1	19.69	-	2	1	20.92	-	22.44	21.29
J090808.2-004610.9	V	0892-0180755			MIS	3	3	17.99	2.47	2	2	18.56	2.88	15.40	14.53
J090904.4+091714.4	T	-			AIS	3	1	17.96	-	2	1	18.11	-	22.33	22.08
J091324.0+091417.9	T	0992-0184047			AIS	3	1	19.93	-	2	1	20.15	-	17.30	15.77
J092458.8+021834.1	T	0923-0226013			AIS	2	1	19.31	-	2	0	-	-	10.83*	10.50*
J092551.9+015545.6	T	0228-01607-1	HD 81463(?)	A0 star	AIS	2	1	17.36	-	2	1	19.70	-	11.79*	14.30*
J092620.4+034541.8	V	0937-0186908			AIS	2	2	17.91	1.88	2	2	18.31	1.95	19.91	19.79
J092851.8+041630.0	V	0942-0172841	FIRST J092851.8+041630	Radio source	AIS	2	2	17.95	1.13	2	2	18.81	0.37	18.66	18.76
J093026.0+071221.6	V	0972-0216018	WW Leo	RR Lyrae-ab	AIS	2	2	15.83	0.97	2	1	19.51	-	12.28*	13.95*
J095801.1+021250.0	V	0922-0237968			DIS	93	2	19.68	3.42	81	1	20.67	-	18.59	17.48
J095816.1+014843.6	T	0918-0208424			DIS	47	1	20.04	-	42	1	21.33	-	21.49	19.92
J100133.3+014328.4	V	0917-0193609		PV	DIS	96	82	17.21	2.00	87	26	19.01	4.85	14.69	14.66
J100141.5+020758.8	V	0921-0232170			DIS	140	97	20.82	2.22	126	10	21.89	1.80	17.60	16.14
J100152.1+021158.5	V	0921-0232199			DIS	93	89	18.80	3.10	84	70	20.62	2.58	13.97	15.86*
J100209.5+020726.5	V	0921-0232253			DIS	93	2	19.58	2.38	84	2	19.73	2.65	21.50	19.99
J100358.9-270001.4	V	0629-0308953			NGS	5	5	18.26	1.43	3	0	-	-	-	-
J102002.7+611538.9	V	1512-0181964			AIS	4	4	16.71	1.62	3	2	19.15	0.85	14.00	14.00
J102525.7-392130.8	V	0506-0220494			NGS	6	6	18.72	1.95	5	2	20.64	0.20	-	-
J104844.1+581539.4	V	1482-0239659		PV	DIS	48	47	18.51	2.88	24	6	19.61	2.45	17.01	16.86
J105513.7+564747.0	V	1467-0226668		PV	DIS	65	62	17.04	2.27	26	9	19.62	2.94	15.50	15.34
J105622.2+570520.6	V	1470-0242660			DIS	62	62	17.02	2.33	26	9	18.06	4.49	15.87	15.60
J105926.1-005927.9	V	0890-0199535	SDSS J105926.11-005927.6	RR Lyrae-ab	DIS	3	3	19.53	2.09	3	1	20.46	-	18.30	18.01
J111147.3+510549.4	V	1410-0219003			AIS	4	4	18.12	1.50	3	1	21.06	-	16.26	15.97
J112334.9+474014.6	V	1376-0264908			AIS	4	4	19.45	1.07	3	0	-	-	17.30	17.05
J113340.3+502328.0	V	1403-0230850	CZ UMa	RR Lyrae-ab	AIS	4	4	16.71	2.93	2	1	17.44	-	14.78	14.91
J114740.7+001521.0	V	0902-0204368	GJ 3685A	dM4e flare	MIS	4	4	13.17	6.67	2	2	13.43	7.69	14.37*	12.84*
J120157.2-183153.7	V	0714-0246553			NGS	5	4	18.83	1.92	5	1	19.87	-	-	-
J122034.6-030947.7	V	0868-0272366			AIS	2	2	19.77	0.51	2	0	-	-	15.05	13.98
J122057.1+673838.9	V	1576-0166067	1RXS J122057.4+673845	x-ray source	MIS	3	3	16.67	1.96	2	2	18.43	3.06	13.29*	11.31*
J122415.6-014914.0	V	0881-0268821	[VZA2004] 195	RR Lyrae	AIS	2	2	19.27	1.34	1	1	20.60	-	16.25	16.41
J122743.3-005754.4	V	0890-0214215	[VZA2004] 199	RR Lyrae	MIS	4	4	19.13	1.82	1	1	20.72	-	17.57	17.32
J122836.9-064230.0	V	0832-0270055			AIS	2	2	19.62	2.39	1	1	20.62	-	-	-
J123313.6+020029.1	V	0920-0259726			NGS	2	2	19.33	1.92	2	1	20.87	-	17.67	17.43
J123349.3-024456.2	V	0872-0322120			MIS	3	3	19.16	1.87	3	1	21.24	-	16.27	16.24
J123512.5+621744.6	T	1522-0247069			DIS	72	1	18.61	-	41	1	18.98	-	19.59	18.07
J123738.0-040841.2	V	0858-0232491			AIS	2	2	18.50	0.94	2	1	21.23	-	-	-
J123913.5-113307.4	V	0784-0251397	NSVS 123913-113314	Radio source	NGS	2	2	17.09	2.33	2	1	17.93	-	-	-
J124109.1+230159.8	T	1130-0231256			AIS	2	1	18.81	-	1	1	20.87	-	-	-
J124328.2-055431.7	T	-			AIS	2	1	19.94	-	1	1	19.56	-	-	-
J124746.2+243940.6	V	1146-0199030			AIS	6	5	18.58	2.25	4	2	19.96	0.77	-	-
J124812.4+005737.4	V	0909-0215691	FASTT 524	variable star	AIS	2	2	18.93	0.95	2	1	21.67	-	16.06	15.86
J124906.9-010421.9	V	0889-0220289	BW Vir	RR Lyrae-ab	MIS	4	3	15.95	2.54	4	2	16.75	0.39	14.03	14.07
J125000.6+310824.0	V	1211-0200416	TX Com	RR Lyrae-ab	AIS	4	4	16.2	1.97	1	1	17.57	-	-	-
J125409.7+252707.8	V	1154-0198874	EN Com	RR Lyrae-ab	AIS	6	4	18.79	1.55	0	0	-	-	-	-
J125428.5+003739.5	V	0291-00256-1			AIS	2	2	16.24	2.61	0	0	-	-	11.91*	11.39*
J125905.7+242632.9	V	1144-0198736			AIS	3	3	17.61	3.67	2	2	17.62	3.04	-	-
J125911.1+263745.1	V	1166-0214036	Ton 682	UV-excess object	AIS	6	4	17.74	0.15	4	4	18.78	1.25	-	-
J130204.5+463533.7	V	1365-0231982			AIS	2	2	18.01	1.45	2	1	19.65	-	15.82	15.85
J130213.6+241420.0	V	1142-0198264	BF Com	RR Lyrae-ab	AIS	2	2	15.55	1.04	2	2	17.3	4.17	-	-
J130615.1+293657.5	V	1196-0208146	EV Com	RR Lyrae-ab	DIS	8	8	19.56	1.91	8	2	21.7	1.62	-	-
J130934.8+285905.9	V	1189-0208615	GJ 1167A	dM5 flare	DIS	6	5	19.44	2.07	3	3	20.66	1.53	-	-
J131012.3+474517.0	V	1377-0296991	1RXS J131011.9+474521		AIS	2	2	19.47	1.24	2	1	21.31	-	15.40	13.79
J131855.8+433100.0	V	1335-0237412			AIS	2	2	18.42	1.33	2	1	21.56	-	16.11	15.87
J132135.3+431145.3	V	1331-0281572			AIS	4	3	18.28	2.27	4	1	19.36	-	16.60	16.38
J132546.6-425140.9	V	0471-0361002			NGS	5	5	18.49	1.78	5	5	19.44	1.58	-	-
J132715.2+425932.1	V	1329-0296231			AIS	4	3	17.88	3.63	4	1	17.67	-	20.81	20.52
J133052.6-031644.6	T	0867-0280752			AIS	2	1	18.63	-	0	0	-	-	22.11	21.02
J133057.0-040824.6	V	0858-0243273			AIS	4	4	16.44	0.56	0	0	-	-	-	-
J133115.8+405657.6	V	1309-0239624			AIS	2	2	16.97	1.41	4	1	18.58	-	14.52	14.50
J133757.1+401610.8	V	1302-0233853			AIS	4	4	20.00	0.91	4	1	21.33	-	18.41	18.34
J134156.2+030744.3	V	0931-0264765			MIS	3	3	17.45	1.41	3	2	20.28	1.04	14.62	14.59
J135408.2+573615.9	V	1476-0290232			AIS	2	2	18.76	1.25	0	0	-	-	15.09	14.74
J140113.3+710524.0	V	1610-0100824			AIS	2	2	16.48	1.91	2	1	18.66	-	-	-
J141755.4+714107.6	V	4406-00241-1			AIS	2	2	16.42	0.70	2	1	21.20	-	-	-
J142329.4+034317.6	V	0937-0238977			MIS	4	2	19.20	2.96	3	1	20.86	-	15.93	14.60
J142551.2+042949.3	V	0944-0225286		UV flare	MIS	7	3	18.62	4.54	5	1	19.21	-	18.88	17.32
J143741.1+344119.0	T	1246-0218818			DIS	84	1	18.40	-	84	1	18.63	-	18.81	17.37
J143753.7+345923.9	V	1249-0218617	ROTSE1 J143753.84+345924.8	RR Lyrae-ab	DIS	84	84	15.79	2.78	84	75	18.23	4.85	13.78*	13.49*
J144433.4+364200.2	V	1267-0242808			AIS	3	2	17.71	1.71	2	2	19.40	0.99	16.14	14.69
J144708.1+345158.4	T	1248-0221943			AIS	6	1	19.50	-	4	1	19.86	-	18.53	17.11
J144738.4+035311.8	V	0938-0240178		UV flare	MIS	3	3	17.83	4.24	3	1	18.48	-	18.02	16.46
J145110.2+310639.7	V	1211-0222759	1RXS J145110.3+310648	x-ray source	DIS	22	21	18.68	0.88	11	10	19.84	0.97	-	-
J145339.2+501151.6	V	1401-0265491			AIS	2	2	18.12	1.48	2	1	19.80	-	16.74	16.48
J150957.7+621334.9	V	1522-0274109			AIS	2	2	18.30	1.97	2	1	20.17	-	14.12	13.36
J151120.0+392036.5	V	1293-0251929			AIS	3	3	16.85	1.22	2	1	18.90	-	14.71	15.38*
J151234.9+392416.1	V	1294-0251325			AIS	3	3	18.44	1.94	2	1	19.75	-	16.22	16.09
J151532.1+364806.4	V	1268-0255264			AIS	3	3	18.78	2.57	2	1	19.90	-	17.42	17.18
J164940.0+345820.3	V	1249-0245815	HL Her	RR Lyrae-ab	DIS	4	4	17.79	1.76	4	2	19.50	2.59	16.11	15.85
J203853.9-580358.6	V	0319-1042594	UU Ind	RR Lyrae-ab	MIS	2	2	16.14	2.50	2	1	17.19	-	-	-
J211517.8+000432.5	V	0900-0581544	SW Aqr	RR Lyrae-ab	MIS	3	3	13.35	2.19	3	3	13.91	6.32	11.77*	11.49*

* = uncertain SSDS magnitude, PV = periodic variable